

1 **DRAFT: Spatiotemporal assessment of *Aprion***
2 ***virescens* density in shallow Main Hawaiian Islands**
3 **waters, 2010-2019.**

4 Kisei R. Tanaka¹, Andrea L. Schmidt^{1,2}, Tye L. Kindinger¹, Jonathan L. Whitney¹ and Jennifer C.
5 Samson¹

- 6 1. Pacific Islands Fisheries Science Center National Marine Fisheries Service 1845 Wasp Boulevard
7 Honolulu, HI 96818
8 2. Cooperative Institute for Marine and Atmospheric Research University of Hawaii 1000 Pope
9 Road Honolulu, Hawaii 96822



11 **U.S. DEPARTMENT OF COMMERCE**
12 **National Oceanic and Atmospheric Administration**

13 National Marine Fisheries Service
14 Pacific Islands Fisheries Science Center

15 NOAA Technical Memorandum NMFS-PIFSC-[##]
16 [https://doi.org/\[...\]](https://doi.org/[...])

17 [Month] [Year]

18 **About this report**

19 The Pacific Islands Fisheries Science Center of NOAA's National Marine Fisheries Service uses
20 the NOAA Technical Memorandum NMFS-PIFSC series to disseminate scientific and technical
21 information that has been scientifically reviewed and edited. Documents within this series reflect
22 sound professional work and may be referenced in the formal scientific and technical literature.

23 **Recommended citation**

24 [Authors]. [Year]. Tech memo template - update title field in file > properties, then right-click
25 this field and select "update." Title should be in sentence-case. U.S. Dept. of Commerce, NOAA
26 Technical Memorandum NMFS-PIFSC-##, 29 p. doi:10...

27 **Copies of this report are available from**

28 Pacific Islands Fisheries Science Center
29 National Marine Fisheries Service
30 National Oceanic and Atmospheric Administration
31 1845 Wasp Boulevard, Building #176
32 Honolulu, Hawaii 96818

33 **Or online at**

34 <https://repository.library.noaa.gov/>

35 Cover: [description and source of optional cover photo]

| | | |
|----|---|---|
| 36 | Table of contents | |
| 37 | DRAFT: Spatiotemporal assessment of <i>Aprion virescens</i> density in shallow Main Hawaiian Islands | |
| 38 | waters, 2010-2019. | 1 |
| 39 | Executive Summary | 7 |
| 40 | Introduction | 7 |
| 41 | Material and methods | 8 |
| 42 | Environmentally enhanced <i>Aprion virescens</i> in situ density data | 8 |
| 43 | Spatiotemporal modeling of changes in <i>Aprion virescens</i> density | 2 |
| 44 | Identification of shallow water <i>Aprion virescens</i> density hotspots using local trends | 3 |
| 45 | Results | 4 |
| 46 | Model fit and selection | 4 |
| 47 | Spatiotemporal dynamics of <i>Aprion virescens</i> density distributions in shallow waters | 1 |
| 48 | Discussion | 1 |
| 49 | References | 3 |
| 50 | Supplemental materials | 1 |
| 51 | | |
| 52 | | |

53 **List of tables**

54 **Table 1. Description of environmental variables included in Aprion virescens density modeling**
55 **effort. CRM: Coastal Relief Model, AquaMODIS: Aqua Moderate Resolution Imaging**
56 **Spectroradiometer, ESA OCCI: European Space Agency Ocean Colour Climate Change**
57 **Initiative, ASCAT: Advanced Scatterometer. 1**

58 **Table 2. The formula for Aprion virescens density includes full and parsimonious models after**
59 **covariate selection. SST: Sea Surface Temperature, ChlA: Chlorophyll_A, SWS: Surface Wind**
60 **Speed. Knots are set at 5 for all continuous predator variables. VIF: Variance Inflation Factor.**
61 **Covariates with VIF > 3 are shown in bold. 1**

62 **Table 3. Summary of predicted Aprion virescens density (individuals per 100 m²) modeling efforts**
63 **in the Main Hawaiian Islands shallow waters, 2010-2019. 2**

64

DRAFT

65 **List of figures**

66 **Figure 1. Fishery-independent (a) size compositions, (b) temporal trends, and (c) spatial**
67 **distributions of *Aprion virescens* density observations in the shallow Main Hawaiian Islands waters**
68 **(0-30 m) for the 2010-2019 period. Data were provided by from the National Coral Reef Monitoring**
69 **Program (www.coris.noaa.gov/monitoring/).** 9

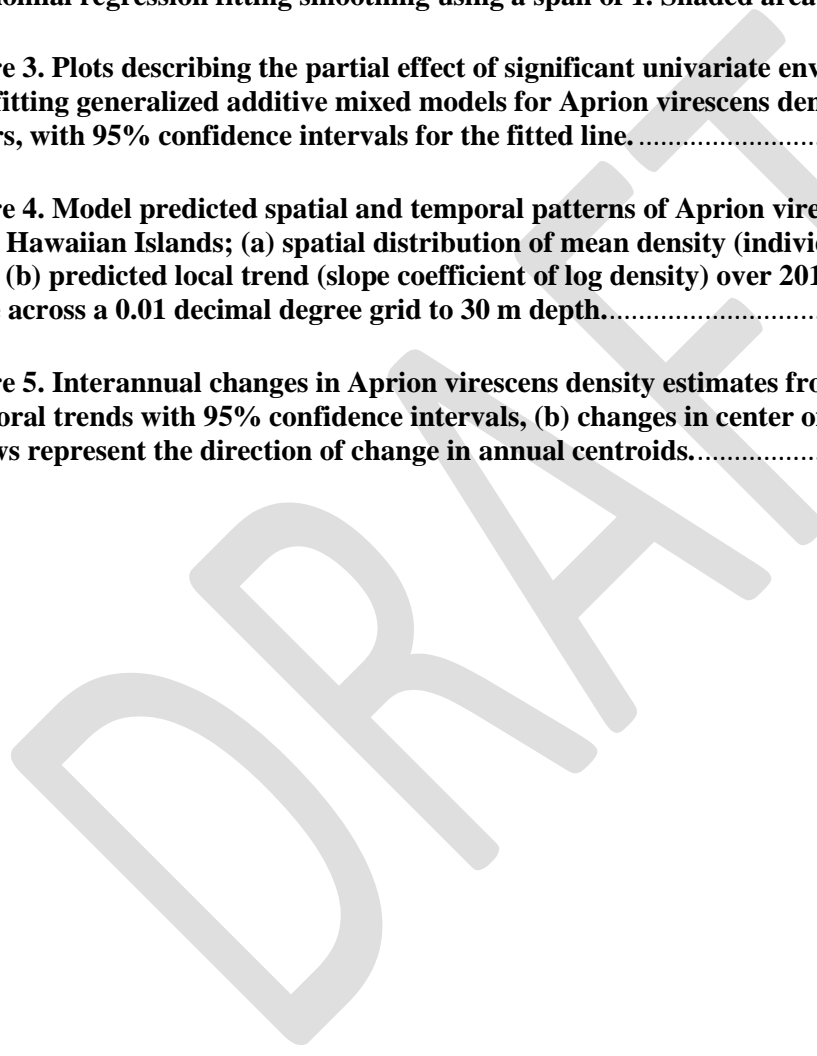
70 **Figure 2. Differences in relative *Aprion virescens* density (y-axis) at temporally-summarized**
71 **environmental gradients in shallow Main Hawaiian Islands waters (0-30 m). Solid line is a local**
72 **polynomial regression fitting smoothing using a span of 1. Shaded area is 95% intervals.**..... 1

73 **Figure 3. Plots describing the partial effect of significant univariate environmental variables in the**
74 **best-fitting generalized additive mixed models for *Aprion virescens* density in the MHI shallow**
75 **waters, with 95% confidence intervals for the fitted line.**..... 1

76 **Figure 4. Model predicted spatial and temporal patterns of *Aprion virescens* density across the**
77 **Main Hawaiian Islands; (a) spatial distribution of mean density (individuals per 100 m²) over 2010-**
78 **2019, (b) predicted local trend (slope coefficient of log density) over 2010-2019. All predictions were**
79 **made across a 0.01 decimal degree grid to 30 m depth.**..... 1

80 **Figure 5. Interannual changes in *Aprion virescens* density estimates from 2010 and 2019: (a)**
81 **temporal trends with 95% confidence intervals, (b) changes in center of gravity (COG), where**
82 **arrows represent the direction of change in annual centroids.**..... 1

83



84 **List of supplemental figures**

85 **Figure S 1. Bathymetric profiles of Aprion virescens density model domain within the Main**
86 **Hawaiian Islands. Bathymetric data were drawn from NOAA Coastal Relief Model, 3 arc second,**
87 **Vol. 10. 1**

88 **Figure S 2. Triangulated mesh covering the Main Hawaiian Islands region prepared with vertices**
89 **at 500 knots using the R INLA package. Axis units are in km based on UTM Zone 4 projection.**
90 **Polygons with blue points represent spatial domains considered for spatial autocorrelations in the**
91 **spatiotemporal generalized linear mixed model calibration process. Polygons with green dots**
92 **represent land masses and were not included in the spatial autocorrelations in the spatiotemporal**
93 **generalized linear mixed model calibration process. 1**

94 **Figure S 3. (a) Graphical summary of model residuals for the season-, stage-, and sex aggregated**
95 **Aprion virescens generalized additive mixed modelling effort, and (b) observed versus predicted**
96 **plots complemented by a linear regression lines. The dashed line represents the 1:1 line and an ideal**
97 **model performance. 2**

98 **Figure S 4. Spatially aggregated changes in Aprion virescens density (2010-2019) within selected**
99 **regional groups. 3**

100

DRAFT

101 **Executive Summary**

102 The Magnuson-Stevens Fishery Conservation and Management Act of 1996 directs regional fishery
103 management councils and the National Marine Fisheries Service (NMFS) to identify and describe
104 “essential fish habitat (EFH)” for all federally managed species to ensure conservation and sustainable
105 management of living marine resources. This report summarizes the statistically-derived density patterns
106 of *Aprion virescens* in shallow coastal waters of the Main Hawaiian Islands (MHIs) from 2010 to 2019. A
107 spatiotemporal modeling technique was used to predict changes in the species' localized density (spatially
108 resolved number of individual estimates per 100 m²) in relation to environmental variables. *A. virescens*
109 densities varied between 0 and 7.27 individuals per 100 m², while several hotspots coinciding with
110 increased density were detected. Changes in *A. virescens* densities over time were best explained by the
111 combination of static (depth) and a dynamic surface oceanographic condition (monthly surface wind
112 speed variability). The geographic center of *A. virescens* density was observed between O‘ahu and
113 Moloka‘i. The observed annual centroids shift was not reflective of a uniform shift in densities but
114 localized changes in density across the MHI shallow waters. Overall, these findings indicate that a
115 spatiotemporal model that can estimate local trends improved the interpretation of species distribution
116 change. The results indicate shallow-water habitats in the MHIs are likely essential for *A. virescens*. The
117 analysis identified existing challenges in determining habitat-use patterns and emphasized the further
118 need for additional systematic sampling to refine the species' distribution patterns within habitats.

119 **Introduction**

120 The Magnuson-Stevens Fishery Conservation and Management Act (Magnuson-Stevens Act) of 1996
121 requires the identification and delineation of essential fish habitat (EFH), defined as “those waters and
122 substrate necessary to fish for spawning, breeding, feeding or growth to maturity” for all species under
123 federal fishery management plans (AN ACT, 1996; Waldeck & Buck, 2001). Under the EFH definition,
124 necessary habitat includes physical, chemical, and biological attributes that support the complete life
125 cycle of a designated species (e.g., egg, larval, juvenile, adult, and spawning adult). The Magnuson-
126 Stevens Act also stipulates that Fisheries Management Plans (FMPs) must “(1) identify and describe
127 EFH, (2) minimize to the extent practicable adverse effects from fishing on EFH and its ability to
128 support fishery ecosystems, and (3) identify other actions to encourage conservation and enhancement
129 of EFH” [16 U.S.C. § 1853(a)(7)]. The biogeography of living marine resources (LMRs) is complex and
130 can vary across space and time (e.g., Álvarez-Noriega et al., 2020). Without environmentally informed
131 EFH delineations, resource managers will be unable to promote a sustainable fishery and healthy marine
132 and freshwater ecosystems. It is, therefore, crucial to (1) develop approaches to monitor and quantify local
133 species-habitat associations, and (2) understand and describe the species’ spatial and temporal variations
134 to incorporate EFH into fisheries management decisions.

135 *Aprion virescens* (common name ‘green jobfish’; Hawaiian name ‘uku’) is a reef-associated
136 snapper most often seen at depths of 0-180 m in tropical coastal Indo-Pacific regions (Franklin, 2021;
137 Froese & Pauly, 2010; Nadon et al., 2020; O’Malley et al., 2021). *A. virescens* is commercially important
138 throughout its geographic range and is often captured using baited handlines and surface trolling lures
139 (Ayers, 2022; Haight et al., 1993; Kelley & Ikehara, 2006). In Hawaii, they are a principal species
140 comprising the deep-slope bottom fish resource across the Hawaiian Archipelago, with a recent annual
141 commercial harvest of 42 tonnes in 2019 (HDAR, 2019). In shallower depths, *A. virescens* are a popular
142 target for spearfishing in the main Hawaiian Islands and elsewhere. A recent benchmark analysis of *A.*
143 *virescens* habitat completed by Nadon et al., (2020) found that the Greater Maui (Maui, Moloka‘i, Lāna‘i,
144 and Kaho‘olawe islands) contained a large portion of the specie’s habitat (58%), followed by Hawaii
145 (23%), O‘ahu (11%), and Kaua‘i- Ni‘ihau (8%) (Nadon et al., 2020).

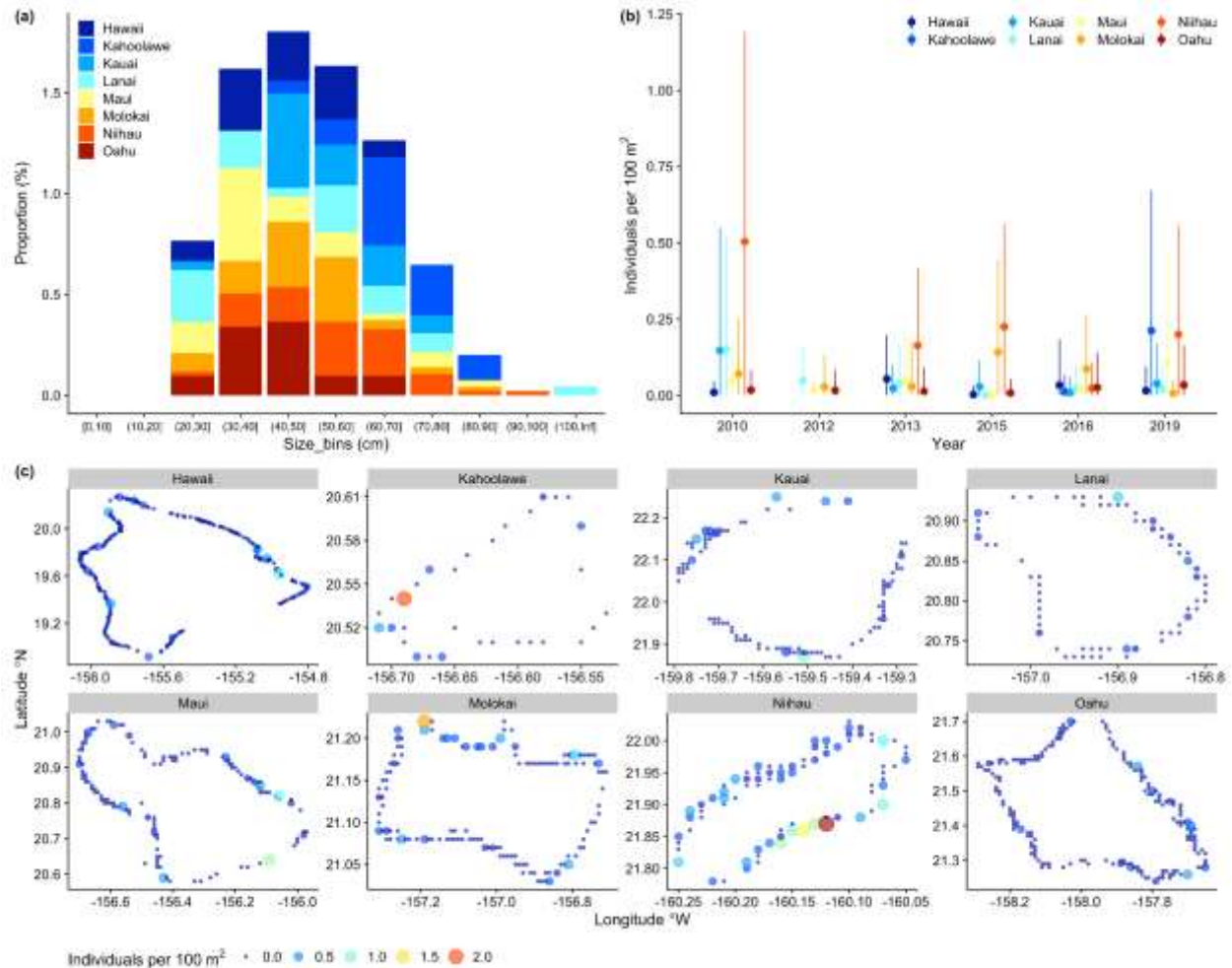
146 The EFH for *A. virescens* is broadly designated from the shoreline to offshore down to 240
147 meters deep (PIRO, 2020), with level 1 EFH projections available (i.e., specie's' presence/absence;
148 Franklin 2021). The need to unify coastal land management with fishery management was reinforced by
149 the EFH provisions in the reauthorization of the 1996 Magnuson-Stevens Act (AN ACT, 1996). Coastal
150 development and nearshore fishing activities in Hawaii may affect multiple aspects of *A. virescens*
151 ecology (Friedlander et al., 2006). At the same time, there are few empirical studies quantifying the
152 species' density (EFH level 2 criterion) in the shallow waters (0-30 m) (e.g., Meyer et al., 2007).
153 Informed fisheries management decisions will likely depend on EFH relevant information, such as
154 whether a target species exhibits an allometric relationship between distribution area and stock biomass.
155 Data gaps hamper ongoing work to define the species' nearshore EFH. More information is needed on the
156 species' habitat utilizations from offshore to nearshore to refine the species' EFH designations in the
157 Main Hawaiian Islands (MHI), a goal identified as a research priority by the Western and Central Pacific
158 Fisheries Commission (WPRFMC, 2021).

159 Under the Magnuson-Stevens Act, the Western Pacific Regional Fishery Management Council
160 (WPFMC) has identified a need for a model-based approach in predicting the distribution of Management
161 Unit Species (MUS) based on multiple habitat-related variables to designate essential fish habitat (EFH)
162 and habitat areas of particular concern (HAPC) for all species included in the Fishery Ecosystem Plans (
163 WPRFMC, 2021). This is particularly crucial and timely in data-poor Pacific regions where shifts in
164 baseline environmental conditions are occurring at an accelerated rate. To this end, we developed a
165 statistical EFH level 2 modeling framework employing a combination of *in-situ* *A. virescens* density data
166 enhanced by various gridded satellite products to estimate the species' abundance in shallow MHI waters.
167 This is the first study to use a large, fishery-independent database as a source of data for analysis and
168 prediction of the habitat distribution of *A. virescens* along the nearshore coastal area in the MHI region.
169 The results of this study provide information on the spatial distribution of *A. virescens*, which fisheries
170 managers can use to distinguish the species' EFH and apply enhanced management strategies.

171 **Material and methods**

172 **Environmentally enhanced *Aprion virescens* in situ density data**

173 The study domain encompasses the shallow (0-30 m) waters around the main Hawaiian Islands.
174 The *in-situ* fishery-independent density observations for *A. virescens* were collected through the National
175 Coral Reef Monitoring Program (NCRMP). The fishery-independent survey was based on a stratified
176 random sampling design using the paired-diver stationary point count (SPC) method (Ayotte et al., 2015;
177 Heenan et al., 2017; McCoy et al., 2019) and collected during daylight hours. This survey occurred from
178 April to December, but primarily from June to October. The SPC diver-based sampling method records
179 fish species, size, and abundance in paired 15-m diameter survey cylinders (353 m²; visually estimated)
180 extending from the seafloor to the surface. These surveys provide site-level density and biomass records
181 across a range of fish species and trophic groups. We used a portion of the survey data collected from 8
182 islands across the MHI region over ten years (2010, 2012-2013, 2015-2016, 2019) at 2968 survey sites
183 (Figure 1). The detailed description of this specific survey can be found in McCoy et al., (2019).



184

185 **Figure 1. Fishery-independent (a) size compositions, (b) temporal trends, and (c) spatial distributions of**
 186 ***Aprion virescens* density observations in the shallow Main Hawaiian Islands waters (0-30 m) for the 2010-**
 187 **2019 period. Data were provided by from the National Coral Reef Monitoring Program**
 188 **(www.coris.noaa.gov/monitoring/).**

189 Relevant environmental variables that are associated with the density distribution of *A. virescens*
 190 were included in the analysis: depth, sea surface temperature (SST), surface chlorophyll-a concentration
 191 (Chl_a), and surface wind speed (SWS) (Figure 2 & Table 1). Temporally corresponding SST, Chl_a,
 192 and SWS values at each surveyed location were obtained for every time-stamped and georeferenced
 193 NCRMP survey record (n=2968) using the Environmental Data Summary (EDS: Tanaka & Oliver 2021).
 194 The resolution of the environmental data was coarser than the expected accuracy of most survey site
 195 locations (<5 km), so horizontal positions were matched to the nearest available gridded data within 0.1°.
 196 Gridded SST data was gathered from the NOAA Daily Global 5km Geo-Polar Blended Sea Surface
 197 Temperature Analysis (v1.0;), which provided daily SST with a resolution of 0.05°. Daily surface Chl_a
 198 concentrations were averaged using two Chlorophyll-a datasets (Aqua MODIS v.2018.0 and ESA OC
 199 CCI v5.0; both at ~0.05° resolution; PML, 2020; Shanmugam, 2011)(Plymouth Marine Laboratory, 2020;
 200 Shanmugam, 2011). The Daily Advanced Scatterometer (ASCAT) Surface Wind Fields Level 3 dataset
 201 was used to derive daily sea surface wind speed with a resolution of 0.25° (Kako et al., 2011). A gridded
 202 bathymetric dataset (~0.0008° resolution) from the NOAA Coastal Relief Model, 3 arc second, Vol. 10
 203 (NGDC, 2005), was used to estimate the depth at each horizontal position. For every dated NCRMP

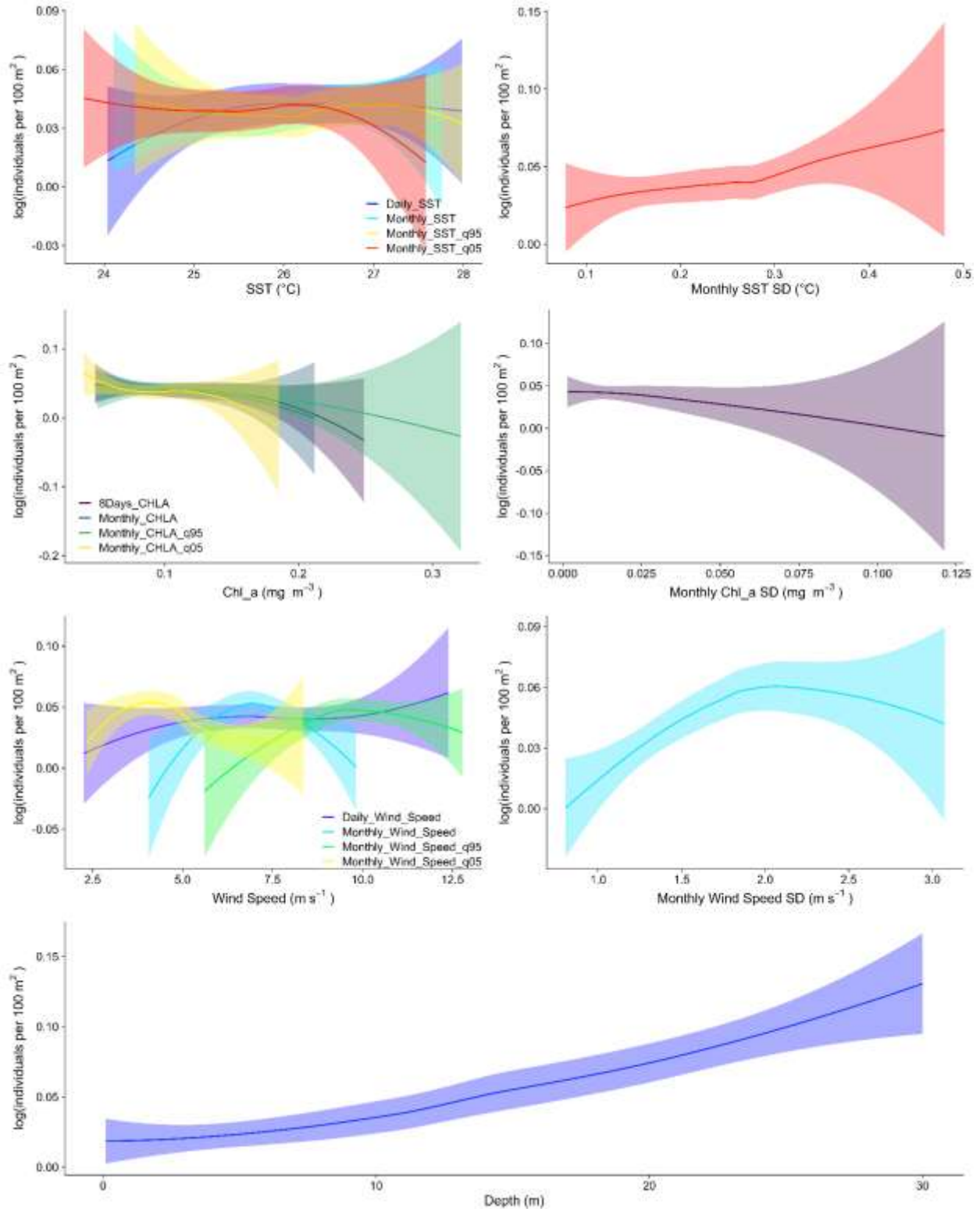
204 survey record, we used EDS to calculate each environmental variable's mean, standard deviation, 5th
205 quantile, and 95th quantile values over the past one month from the corresponding survey date.

DRAFT

206 **Table 1. Description of environmental variables included in *Aprion virescens* density modeling effort. CRM: Coastal Relief Model, AquaMODIS: Aqua**
 207 **Moderate Resolution Imaging Spectroradiometer, ESA OCCI: European Space Agency Ocean Colour Climate Change Initiative, ASCAT: Advanced**
 208 **Scatterometer.**

| Dataset | Description | Temporal range | Spatial scale | Sources | Unit |
|-------------------------------------|---------------------------------------|----------------|---------------|------------|--------------------|
| Bathymetry_CRM | Ocean depth | n/a | 0.0008° | Coastwatch | m |
| Chlorophyll A AquaMODIS | Sea surface chlorophyll concentration | 8day | 0.04° | Oceanwatch | mg m ⁻³ |
| Chlorophyll A ESA OCCI | Sea surface chlorophyll concentration | 8day | 0.04° | Oceanwatch | mg m ⁻³ |
| ASCAT Level 3 | Sea surface wind speed | Daily | 0.25° | Oceanwatch | m s ⁻¹ |
| NOAA Geo-Polar Blended SST Analysis | Sea surface temperature | Daily | 0.05° | Oceanwatch | °C |

DRAFT



209

210 **Figure 2. Differences in relative *Aprion virescens* density (y-axis) at temporally-summarized environmental**
 211 **gradients in shallow Main Hawaiian Islands waters (0-30 m). Solid line is a local polynomial regression fitting**
 212 **smoothing using a span of 1. Shaded area is 95% intervals.**

213 Spatiotemporal modeling of changes in *Aprion virescens* density

214 We estimated localized changes in the distribution of *A. virescens* density in relation to dynamic
215 environmental variables using a spatiotemporal model. Spatiotemporal models are becoming increasingly
216 popular in ecology. The approach incorporates a spatially explicit temporal trend (i.e., local trend)
217 alongside spatial (temporally constant) and spatiotemporal (time-varying) components, thereby imposing
218 correlation across space and time in the estimates of target response variables. Using this approach, *A.*
219 *virescens* density is modeled as a function of ‘fixed’ effects resulting from explicit habitat variables and
220 random effects as a product of unobserved or ‘latent’ spatiotemporal effects using Gaussian Markov
221 random fields. Accounting for spatial autocorrelation between spatially referenced observations
222 proximate in both space and time can derive biogeographical signals for evaluating the species’ habitat
223 preference in shallow water.

224 We applied a statistical mixed-modeling approach (generalized additive mixed-effect model;
225 GAMM) that accounts for spatial autocorrelation between spatially referenced observations and effects of
226 environmental drivers. While *A. virescens* is large (up to 112 cm total length), long-lived (up ~30 years
227 old), and reaches sexual maturity at age 4 (Nadon et al., 2020), we modeled the density of all size bins
228 and year class combined as the species exhibits low density across the MHI islands (mean 0.05, max 2.26
229 individuals per 100 m²), we chose density over biomass as it is more relevant to the species’ stock
230 assessment (Nadon et al., 2020).

231 We used the R *sdmTMB* package (Anderson et al., 2022; Barnett et al., 2021) to fit a full
232 spatiotemporally explicit GAMM with a local trend to estimate size-aggregated *A. virescens* density
233 through space and time. The *sdmTMB* package provides a flexible mixed modeling framework that
234 incorporates an automatic differentiation platform, which fits models by finding the minimum log
235 likelihood based on *nlminb* optimization routine (Kristensen, 2014). We included both spatial and
236 spatiotemporal components. Sampling year was included as a factor (estimating a separate mean per year)
237 to account for annual fluctuations in density. Environmental variables used to predict *A. virescens* density
238 (e.g., depth and temperature) are often correlated. Variance inflation factors (VIFs) were therefore
239 calculated, and variables with VIF value > 3 were removed to minimize collinearity (Table 1; Tanaka et
240 al., 2017; Zuur et al., 2007). The full models were fitted with the VIF-filtered covariates (fixed year
241 effects and five environmental covariates). We used thin plate regression splines with fixed basis
242 dimensions to allow for a smooth relationship between some predictors and the response variable. *A.*
243 *virescens* density data contained zero and continuous positive values. Therefore we used a Tweedie
244 distribution model with a log link. This setting has been shown to perform well with zero-inflated data
245 (Barnett et al., 2021; Tanaka et al., 2018; Tweedie, 1984). The full model can be written as follows:

$$y_{s,t} \sim \text{Tweedie}(\mu_{s,t}, \rho, \Phi), 1 < \rho < 2,$$

$$\mu_{s,t} = \exp(\alpha_t + \beta E_{s,t} + \omega_s + \epsilon_{s,t} + \zeta_s t),$$

$$\omega \sim \text{MVNormal}\left(0, \sum_{\omega}\right),$$

$$\epsilon_t \sim \text{MVNormal}\left(0, \sum_{\epsilon}\right),$$

$$\zeta \sim MVNormal\left(0, \sum_{\zeta}\right),$$

246

Equation 1.

247 where $y_{s,t}$ is *A. virescens* density (individuals per 100 m²) at location s and time t , μ is the mean *A.*
 248 *virescens* density at location s and time t , ρ is the Tweedie power parameter that varies between 1 and 2,
 249 and φ is the dispersion parameter. The α_t is estimated independently for each year. The β is an
 250 environmental covariate. ω_s and $\epsilon_{s,t}$ are spatial and spatiotemporal random effects, respectively, derived
 251 from Gaussian Markov random fields (Cressie and Wikle 2015) with respective covariance matrices \sum_{ϵ}
 252 and \sum_{ω} . The ζ_{st} are the spatially varying coefficients that capture local trends through time (i.e., 2010-
 253 2019), also derived from Gaussian Markov random fields. Time, t (i.e., year), is incorporated after
 254 multiplying with ζ_s and centered by its mean value. All random fields incorporate covariance matrices
 255 constrained by anisotropic Matérn covariance functions with independent scales but share the same κ
 256 parameters controlling the decay rate of spatial correlation as a function of distance (Thorson, 2019;
 257 Wikle et al., 2019). Using the INLA package, the continuous random fields with triangulated mesh were
 258 prepared with vertices at 500 knots (Figure S2). The random fields account for spatial and temporal
 259 autocorrelation between sampling events and estimate unmeasured components of *A. virescens* habitat
 260 suitability (i.e., relative density), allowing that suitability to change through time. The models estimate a
 261 spatiotemporal random field that controls for remaining correlated spatial correlation processes each year
 262 that are not accounted for by the fixed effects. This random field follows a stationary autoregressive
 263 (AR1) process with a first-order correlation. Conventional diagnostic plots (quantile-quantile plot) and
 264 spatial patterns in residuals were examined to analyze model fits (Figure S3).

265 Identification of shallow water *Aprion virescens* density hotspots using local 266 trends

267 We predicted *A. virescens* density at each grid location defined by NOAA CRM bathymetry data
 268 (originally at 3 arc seconds, ~90 m but aggregated to .01 decimal degrees) to develop a smooth surface of
 269 density estimates across the study domain. Predictions of the density of *A. virescens* were based on all
 270 fixed and random effects for each year. To investigate annual variability in the spatial distribution of *A.*
 271 *virescens*, we generated maps of mean predicted density (individuals per 100 m²) from 2010 to 2019. We
 272 use the mean predicted density and localized linear trends over time as a benchmark for describing how *A.*
 273 *virescens* density distributions change. To provide a metric for comparing annual differences in the
 274 distribution of abundance, we estimated the center of gravity (COG) from predicted densities y for each
 275 location s and time t ;

$$COG_t = \frac{\sum y_{st} L_s}{\sum Y_{st}}$$

276

Equation 2

277 where L_s is the y coordinate Y_{st} of location s . The COG is an important ecological indicator that describes
 278 the average latitudinal and longitudinal centers of the population (Friedland et al., 2021; Tanaka et al.,
 279 2018). All analyses were performed in the R programming environment (ver. 4.0.1.; R Core Team, 2021;
 280 <www.r-project.org>). Reproducible R scripts and data can be found in github.com/krtanaka/pifsc_efh.

281 **Results**

282 **Model fit and selection**

283 Candidate predictors with VIF values > 3 were omitted before fitting a GAMM (Table 1).
284 Stepwise backward selection using chi-square statistical tests and Akaike's information criteria (AIC) was
285 used to reduce a post-VIF full model to a parsimonious model with lowest AIC and only significant
286 variables (Tanaka et al., 2018). The inclusion of depth and monthly surface wind variability as predictors
287 yield the parsimonious model identified by the AIC-based model selection procedure (Table 2). The
288 addition of monthly surface wind variability showed a substantial decrease in AIC from the Post-VIF full
289 model (ΔAIC 7, Table 2) therefore included in the parsimonious model. Based on AIC and inspection of
290 residuals (Figure S3a), the rest of the results will focus on analyzing the parsimonious model. The cross-
291 validation result suggested that the final model can predict that the model performance was close to being
292 ideal (1:1 slope; Figure S3b); however, variability in model accuracy increased at higher density (Figure
293 S3b).

DRAFT

294 **Table 2. The formula for *Aprion virescens* density includes full and parsimonious models after covariate selection. SST: Sea Surface Temperature,**
 295 **ChlA: Chlorophyll_A, SWS: Surface Wind Speed. Knots are set at 5 for all continuous predator variables. VIF: Variance Inflation Factor. Covariates**
 296 **with VIF > 3 are shown in bold.**

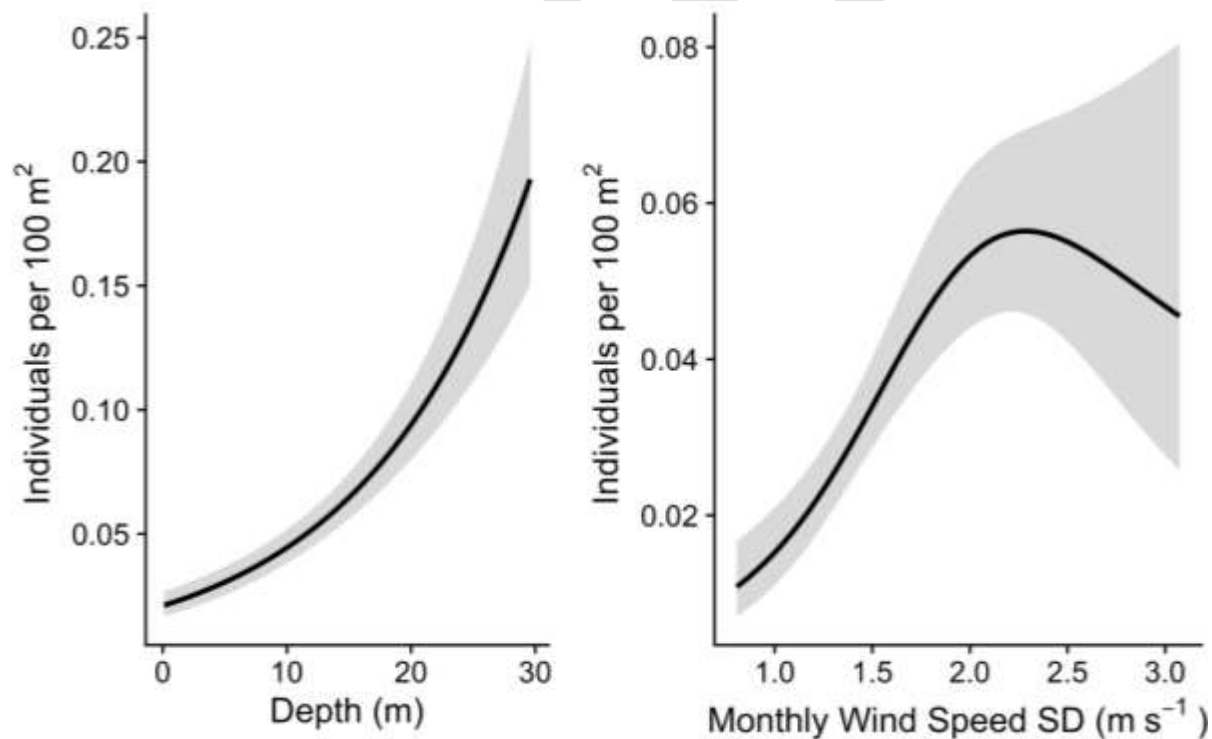
| Level | Predictors | AIC |
|----------------------|---|-------|
| Pre-VIF global model | Year + s(depth) + s(daily_SST) + s(8day_ChIA) + s(daily_SWS) + s(monthly_mean_SST) + s(monthly_mean_ChIA) + s(monthly_mean_SWS) + s(monthly_95th_quantile_SST) + s(monthly_5th_quantile_SST) + s(monthly_95th_quantile_ChIA) + s(monthly_5th_quantile_ChIA) + s(monthly_95th_quantile_SWS) + s(monthly_5th_quantile_SWS) + s(monthly_SST_SD) + s(monthly_ChIA_SD) + s(monthly_SWS_SD) | n/a |
| Post-VIF full model | Year + s(depth) + s(daily_SST) + s(daily_SWS) + s(monthly_mean_SWS) + s(monthly_5th_quantile_ChIA) + s(monthly_SST_SD) + s(monthly_ChIA_SD) + s(monthly_SWS_SD) | 682.3 |
| Parsimonious model | Year + s(depth) + s(monthly_SWS_SD) | 675.4 |

DRAFT

297 **Spatiotemporal dynamics of *Aprion virescens* density distributions in shallow**
298 **waters**

299 Response curves for *A. virescens* density as a function of depth and monthly surface wind
300 variability (SD) were linear and dome-shaped, respectively, with higher density were predicted at deeper
301 and higher wind speed variability (Figure 3). The predicted *A. virescens* density varied from 0 to 7.27
302 individuals per 100 m² from 2010 to 2019, where the lowest mean density was found in O‘ahu ($\mu = 0.02$,
303 $\sigma = 1.2 \cdot 10^{-4}$), and the highest was from Ni‘ihau and Kaua‘i islands ($\mu = 0.1$, $\sigma = 7.9 \cdot 10^{-4}$) (Table 3 &
304 Figure 4a). The highest mean predicted density was found in the Ni‘ihau-Kaua‘i region, while O‘ahu was
305 characterized with the lowest predicted density. Predictions from the parsimonious model show fine-scale
306 spatial structures in rates of changes of *A. virescens* density across the MHI region (Figure 4b). An
307 increase in density was most pronounced in the southwest corners of Ni‘ihau and Kaua‘i, while overall
308 decreasing trends were found across the MHI region (Figure S4). Note that these density distributions
309 extend deeper than 30 m, and findings from these analyses only describe the dynamics of density
310 distribution within the MHI survey domain of 0-30 m.

311 From 2010 to 2019, mean *A. virescens* density varied between 0.02 and 0.15 individuals per 100
312 | m² while linear trends varied from -0.065 (O‘ahu) to 0.041 year⁻¹ (Ni‘ihau-Kaua‘i) (Figure 5a). No
313 significant trends were found over time in any sub-regional groups (Figure 5a). The geographic center of
314 *A. virescens* density showed moderate interannual variability between O‘ahu and Moloka‘i, where the
315 largest COG shift occurred between 2015 and 2016 (Figure 5b). The observed shift over time in the COG
316 | is not reflective of a uniform shift in densities, but likely reflects localized changes in density in MHI
317 islands (e.g., Maui and Hawai‘i).



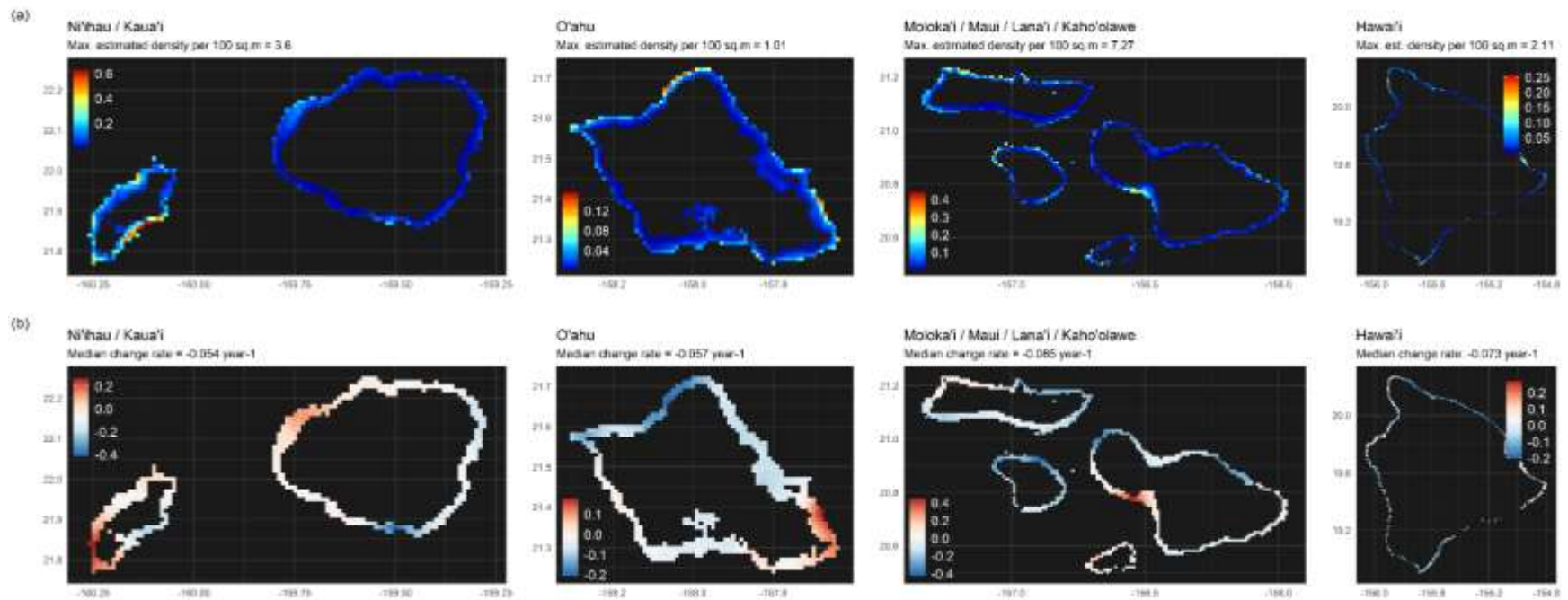
318

319 **Figure 3. Plots describing the partial effect of significant univariate environmental variables in the best-**
320 **fitting generalized additive mixed models for *Aprion virescens* density in the MHI shallow waters, with 95%**
321 **confidence intervals for the fitted line.**

322 **Table 3. Summary of predicted *Aprion virescens* density (individuals per 100 m²) modeling efforts in the Main**
323 **Hawaiian Islands shallow waters, 2010-2019.**

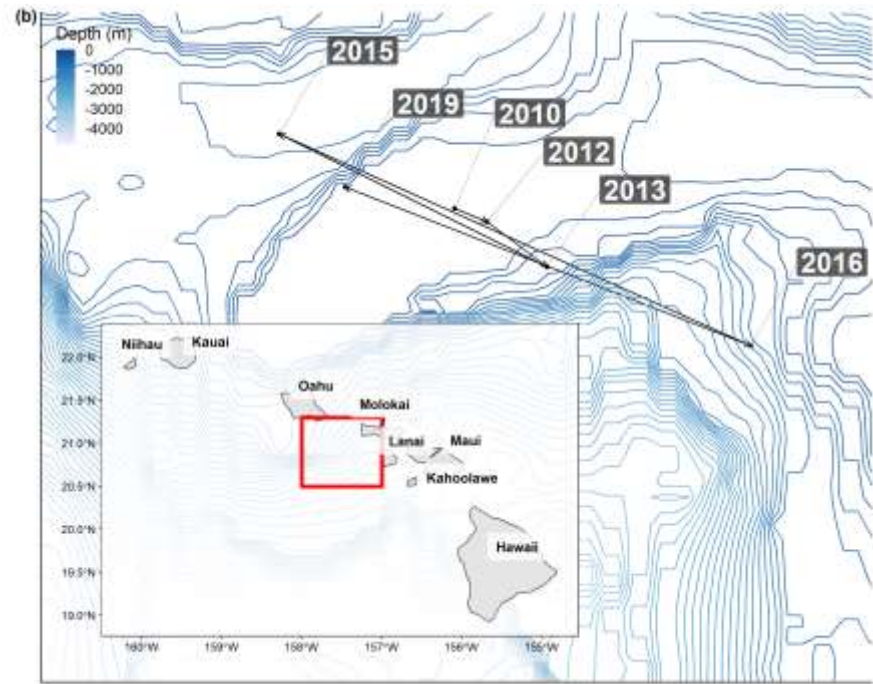
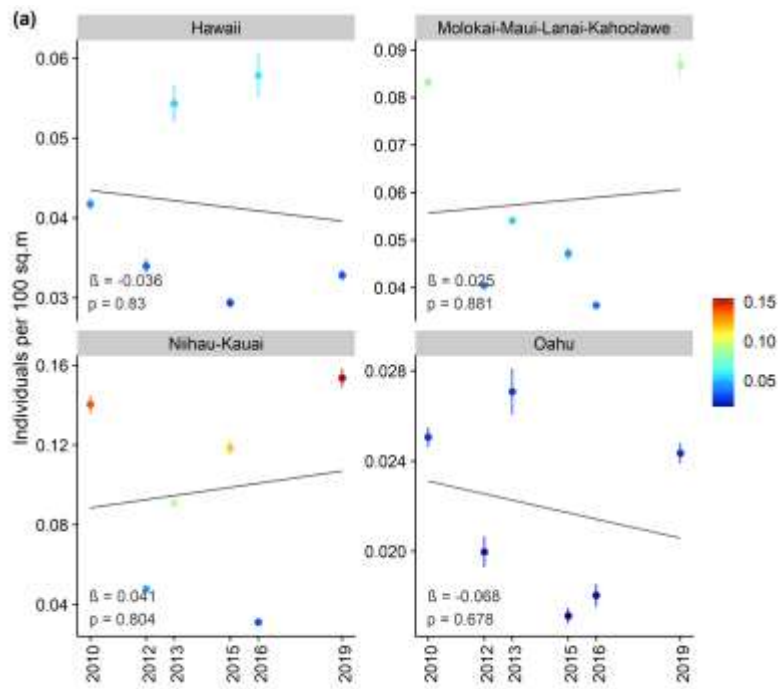
| Islands | Max | Mean | SE |
|---------------------------------|------|------|----------|
| Ni‘ihau-Kaua‘i | 3.6 | 0.1 | 0.000791 |
| O‘ahu | 1.01 | 0.02 | 0.000122 |
| Moloka‘i-Maui-Lāna‘i-Kaho‘olawe | 7.27 | 0.06 | 0.000346 |
| Hawai‘i | 2.11 | 0.04 | 0.000355 |

DRAFT



324

325 **Figure 4. Model predicted spatial and temporal patterns of *Aprion virescens* density across the Main Hawaiian Islands; (a) spatial distribution of mean**
 326 **density (individuals per 100 m²) over 2010-2019, (b) predicted local trend (slope coefficient of log density) over 2010-2019. All predictions were made**
 327 **across a 0.01 decimal degree grid to 30 m depth.**



328

329 **Figure 5. Interannual changes in *Aprion virescens* density estimates from 2010 and 2019: (a) temporal trends with 95% confidence intervals, (b) changes**
 330 **in center of gravity (COG), where arrows represent the direction of change in annual centroids.**

331 Discussion

332 Few studies have characterized *A. virescens* EFH (Franklin, 2021; Meyer et al., 2007). In the
333 MHI, the species is considered a habitat generalist and displays wide distribution coupled with various
334 habitat ranges, including shallow-water reefs, insular shelves, and deep-water slopes between 20 m and
335 180 m (O'Malley et al., 2021). The predicted abundance estimates were coherent with those obtained in
336 previous studies in the MHI (e.g., Franklin, 2021; Nadon et al., 2020). A recent analysis of *A. virescens*
337 habitat found that the Maui Nui complex hosts a large portion of the species' habitat in the MHI, where
338 our density modeling also showed higher density in Ni'ihau, Moloka'i, and Maui ($\max = 7.27$, $\mu = 0.06$, σ
339 $= 0.000346$; Figure 4a). While we found generally low *A. virescens* density (< 0.05 individuals per 100
340 m^2) across the shallow MHI waters, the density COGs were found near Penguin Bank (-11.42°N
341 175.5°W ; Figure 5b), implying that the species density in shallow waters was predicted across the study
342 domain. The density modeling of *A. virescens* revealed a significant linear positive relationship with
343 depth and a tendency for *A. virescens* density to be highest toward deeper waters (Figure 3). This finding
344 agrees with a recent EFH level 1 (presence-absence) analysis conducted at a larger spatial scale (Franklin,
345 2021). The conventional model selection indicates that common oceanographic variables such as
346 chlorophyll-a concentration (Chl-a) and sea surface temperature (SST) were less useful or statistically
347 unrelated. The mixed additive modeling approach revealed a quantified additive influence of dynamic and
348 static environmental covariates. Higher *A. virescens* density was more likely to be observed in deeper
349 waters when surface wind variability over the past month is high (Figure 3). However, the predicted
350 patterns in *A. virescens* density found in this study does not necessarily imply an overall population
351 ecology at the regional level (i.e., species whole distribution range across MHI), and the density-
352 environment relationship found in this study should be treated with caution as individuals from
353 unsampled areas (areas with depth > 30 m) were not incorporated in our density modeling. For example,
354 the deeper depth ranges of Penguin Bank are considered the species' core habitats (25% interquartile
355 range of predicted occurrence), but were outside of this study's spatial scope (Franklin, 2021).

356 Federal and state agencies are tasked with conducting population and habitat assessments for
357 living marine resources (LMR) using the best available data and models. We used spatiotemporal
358 modeling of geographically comprehensive fishery-independent data to derive the first-ever model-based
359 density estimates of a bottom-fish Management Unit Species across the MHI shallow waters.
360 Spatiotemporal models that reflect LMR distributions, such as those used here, can be harnessed to
361 understand large-scale patterns and processes that drive LMR habitat use (Brodie et al., 2020; Evans et
362 al., 2021). This information may be used to enhance indices of relative abundance that serve as proxies
363 for the CPUE, which is commonly used as the index in stock assessment modeling and in determining
364 stock abundance status (Cao et al., 2017; Thorson et al., 2015). Our study also establishes a way to
365 account for uneven sampling effort and incorporate habitat condition information, including
366 oceanographic indices as demonstrated here, into a target species density estimate. Local environmental
367 variables, such as SST and Chl-a considered in this study, were often unavailable to capture complex
368 associations between environment and ecological process due to original survey designs and time lags in
369 species responses coupled with the non-linear intrinsic nature of population dynamics (Hallett et al.,
370 2004). This approach includes temporarily summarized habitat conditions as additional covariates to
371 explain variation in groundfish spatiotemporal density (Tanaka and Oliver 2021). The methodology
372 developed in this study is applicable to other regions where commercially important fish span areas
373 monitored by multiple scientific surveys. This type of information is critical in developing informed
374 management strategies such as marine spatial planning (Evans et al., 2021). This study presents the first
375 step towards incorporating the physical and climate variables that lead to the development of dynamic
376 EFH analysis, with the ultimate goal of delineating EFH across the MHI region.

377 However, as with any modeling exercise, some caution should be exercised when interpreting the
378 results. The analysis was restricted to fishery-independent data to provide statistically comparable density
379 estimates in shallow-water areas. Existing diver and camera surveys providing information on species
380 abundance in this region have large temporal gaps, meaning that these data may not accurately represent
381 the target species' ecology. For example, the NCRMP survey covers a broad spatial range but lacks
382 seasonality data, as it only covers a fraction of the surveyed year. *A. virescens* exhibits a strong
383 seasonality characterized by the summer spawning season (Everson et al., 1989) and winter-summer
384 migrations (Meyer et al., 2007). Furthermore, the NCRMP sampling design targets hard bottom and reef-
385 associated fishes (McCoy et al., 2019), while *A. virescens* is known to utilize soft bottom, low rugosity
386 habitat, and the transition between the two (Whitney, *per.comm*), meaning that NCRMP surveys likely
387 provide an incomplete understanding of the species' affinity for seasonally-dependent habitats. In
388 addition, as our focus was on size and sex aggregated *A. virescens* density changes, phenological
389 differences between life stages, such as shifts in habitat preferences between juvenile and adult stages
390 (Tanaka et al., 2018), were not addressed. Current work on habitat preferences of early life stages is
391 limited and most *A. virescens* larvae sampling sites occur in the water-column and do not overlap with
392 those covered by NCRMP surveys. The smallest individual *A. virescens* detected in NCRMP visual
393 surveys was 22 cm (Whitney, *per. comm*), and therefore the underlying dataset does not characterize
394 juvenile stages. For early life stages, previous definitions of *A. virescens* EFH assumed that larval depth
395 was limited to the lower limit of the adult habitat (WPRFMC, 2011). Analyses of depth integrated
396 ichthyoplankton tows taken offshore of Oahu in 1985-1986 suggest a maximum depth of 40m for larvae
397 between 2 and 6.5 mm in length (Schmidt, *per. comm*; Boehlert & Mundy, 1996). Habitat preferences and
398 distribution patterns for early life stages, particularly larger larvae and pelagic juveniles remains unknown
399 as individuals these sizes (~3-9cm) are absent from collections or available survey data. This knowledge
400 gap limits our understanding of the pelagic and benthic habitats used during the first year after hatching.
401 Studies on juvenile *A. virescens* benthic habitat preferences are also extremely limited. A single juvenile
402 has been found in a flat hard bottom area with *Halimeda sp.* stands (Parrish, 1989). In a separate study
403 focused on adults, the single sexually immature individual in the study appeared to have high residency at
404 the site in question (Filous et al., 2017). Future research should focus on (1) understanding habitat use of
405 early life stages (<9cm) especially surveys of larvae in nearshore water column and juveniles
406 transitioning from pelagic to benthic habitat; (2) quantifying environmental effects on the species'
407 relevant life cycle phases and (3) improving links between response variables' spatial and temporal scales
408 with environmental predictors. These factors would likely improve the utility of EFH model outputs and
409 may result in an improved understanding of environmental variables driving *A. virescens* distribution
410 throughout their life cycle.

411 Currently, there is a lack of information on the influence of environmental variables or abiotic
412 factors (e.g., depth, temperature, oxygen) on the spatiotemporal distribution of MUS. Diverse information
413 sets are necessary to manage EFH and protected areas involving multispecies fisheries. The previous
414 review panel's recommendations included increasing efforts to monitor and record various *in situ*
415 environmental variables (e.g., bottom water temperature and salinity) in fishery-independent surveys.
416 Calibrating historical data and coordinating future data collection efforts to fully understand and manage
417 changing density and shifting distribution of fish species can serve as platforms to synthesize the ecology
418 of these MUS.

419 **References**

- 420 Álvarez-Noriega, M., Burgess, S. C., Byers, J. E., Pringle, J. M., Wares, J. P., & Marshall, D. J. (2020).
421 Global biogeography of marine dispersal potential. *Nature Ecology & Evolution*, *4*(9), 1196–1203.
- 422 AN ACT. (1996). *Magnuson-Stevens Fishery Conservation and Management Act. Public Law, 94: 265.*
- 423 Anderson, S. C., Ward, E. J., English, P. A., & Barnett, L. A. K. (2022). sdmTMB : an R package for fast
424 , flexible , and user-friendly generalized linear mixed effects models with spatial and spatiotemporal
425 random fields. *BioRxiv*, 1–17.
- 426 Ayers, A. L. (2022). *Ecosystem & Socioeconomic Profile of uku (Aprion virescens) in the main Hawaiian*
427 *Islands* (Issue January).
- 428 Ayotte, P., Mccoy, K., Heenan, A., Williams, I., & Zamzow, J. (2015). *Coral Reef Ecosystem Division*
429 *Standard Operating Procedures: Data Collection for Rapid Ecological Assessment Fish Surveys.*
430 <https://doi.org/10.7289/V5SN06ZT>
- 431 Barnett, L. A. K., Ward, E. J., & Anderson, S. C. (2021). Improving estimates of species distribution
432 change by incorporating local trends. *Ecography*, *44*(3), 427–439.
433 <https://doi.org/10.1111/ecog.05176>
- 434 Boehlert, G. W., & Mundy, B. C. (1996). *Ichthyoplankton vertical distributions near Oahu, Hawaii,*
435 *1985-1986: data report.*
- 436 Brodie, S. J., Thorson, J. T., Carroll, G., Hazen, E. L., Bograd, S., Haltuch, M. A., Holsman, K. K.,
437 Kotwicki, S., Samhoury, J. F., & Willis-Norton, E. (2020). Trade-offs in covariate selection for
438 species distribution models: a methodological comparison. *Ecography*, *43*(1), 11–24.
- 439 Cao, J., Thorson, J. T., Richards, R. A., & Chen, Y. (2017). Spatio-temporal index standardization
440 improves the stock assessment of northern shrimp in the Gulf of Maine. *Canadian Journal of*
441 *Fisheries and Aquatic Sciences*, *74*(11), 1781–1793. <https://doi.org/10.1139/cjfas-2016-0137>
- 442 Evans, R., English, P. A., Anderson, S. C., Gauthier, S., & Robinson, C. L. K. (2021). Factors affecting
443 the seasonal distribution and biomass of *E. pacifica* and *T. spinifera* along the Pacific coast of
444 Canada: A spatiotemporal modelling approach. *PLoS ONE*, *16*(5 May), 1–21.
445 <https://doi.org/10.1371/journal.pone.0249818>
- 446 Everson, A. R., Williams, H. A., & Ito, B. M. (1989). Maturation and reproduction in two Hawaiian
447 eteline snappers, uku, *Aprion virescens*, and onaga, *Etelis coruscans*. *Fishery Bulletin*, *87*(4), 877–
448 888.
- 449 Filous, A., Friedlander, A., Wolfe, B., Stamoulis, K., Scherrer, S., Wong, A., Stone, K., & Sparks, R.
450 (2017). Movement patterns of reef predators in a small isolated marine protected area with
451 implications for resource management. *Marine Biology*, *164*(1), 1–16.
- 452 Franklin, E. C. (2021). *Model-based Essential Fish Habitat Definitions for the Uku Aprion virescens in*
453 *the Main Hawaiian Islands by.*
- 454 Friedland, K. D., Smoliński, S., & Tanaka, K. R. (2021). Contrasting patterns in the occurrence and
455 biomass centers of gravity among fish and macroinvertebrates in a continental shelf ecosystem.
456 *Ecology and Evolution*, *October 2020*, 2050–2063. <https://doi.org/10.1002/ece3.7150>
- 457 Friedlander, A. M., Brown, E., Monaco, M. E., & Clarke, A. (2006). *Fish habitat utilization patterns and*
458 *evaluation of the efficacy of marine protected areas in Hawaii: integration of NOAA digital benthic*
459 *habitat mapping and coral reef ecological studies.*
- 460 Froese, R., & Pauly, D. (2010). *FishBase*. Fisheries Centre, University of British Columbia.
- 461 Haight, W. R., Parrish, J. D., & Hayes, T. A. (1993). Feeding ecology of deepwater lutjanid snappers at

462 Penguin Bank, Hawaii. *Transactions of the American Fisheries Society*, 122(3), 328–347.

463 Hallett, T. B., Coulson, T., Pilkington, J. G., Clutton-Brock, T. H., Pemberton, J. M., & Grenfell, B. T.
 464 (2004). Why large-scale climate indices seem to predict ecological processes better than local
 465 weather. *Nature*, 430(6995), 71–75.

466 Hawaii Division of Aquatic Resources (HDAR). (2019). *COMMERCIAL MARINE LANDINGS*
 467 *SUMMARY TREND REPORT* (p. 17). <https://dlnr.hawaii.gov/dar/files/2021/04/cmlstr2019.pdf>

468 Heenan, A., Williams, I. D., Acoba, T., DesRochers, A., Kosaki, R. K., Kanemura, T., Nadon, M. O., &
 469 Brainard, R. E. (2017). Data Descriptor: Long-term monitoring of coral reef fish assemblages in the
 470 Western central pacific. *Scientific Data*, 4, 1–13. <https://doi.org/10.1038/sdata.2017.176>

471 Kako, S., Isobe, A., & Kubota, M. (2011). High-resolution ASCAT wind vector data set gridded by
 472 applying an optimum interpolation method to the global ocean. *Journal of Geophysical Research:*
 473 *Atmospheres*, 116(D23).

474 Kelley, C., & Ikehara, W. (2006). The impacts of bottomfishing on Raita and west St. Rogatien banks in
 475 the Northwestern Hawaiian Islands. *Atoll Research Bulletin*.

476 Kristensen, K. (2014). *General random effect model builder tool inspired by ADMB* (p. 13).

477 McCoy, K., Asher, J., Ayotte, P., Gray, A., Kindinger, T., & Williams, I. (2019). *Pacific Reef Assessment*
 478 *and Monitoring Program Data Report - Ecological monitoring 2019 - Reef fishes and benthic*
 479 *habitats of the main Hawaiian Islands: PIFSC data report DR-19-039*.
 480 <https://doi.org/10.25923/he4m-6n68>

481 Meyer, C. G., Papastamatiou, Y. P., & Holland, K. N. (2007). Seasonal, diel, and tidal movements of
 482 green jobfish (*Aprion virescens*, Lutjanidae) at remote Hawaiian atolls: Implications for marine
 483 protected area design. *Marine Biology*, 151(6), 2133–2143. [https://doi.org/10.1007/s00227-007-](https://doi.org/10.1007/s00227-007-0647-7)
 484 [0647-7](https://doi.org/10.1007/s00227-007-0647-7)

485 Nadon, M. O., Sculley, M., & Carvalho, F. (2020). *Stock assessment of Uku (Aprion virescens) in Hawaii,*
 486 *2020. May*, 120.

487 National Geophysical Data Center (NGDC). (2005). *Coastal Relief Model Vol.10 - Hawaii*. National
 488 Centers for Environmental Information, NESDIS, NOAA, U.S. Department of Commerce.
 489 <https://doi.org/10.7289/V5RF5RZZ>

490 O'Malley, J., Wakefield, C. B., Kinney, M. J., & Newman, S. J. (2021). Markedly Similar Growth and
 491 Longevity of Green Jobfish *Aprion virescens* over an Expansive Geographic Range between the
 492 Hawaiian Archipelago and the Eastern Indian Ocean. *Marine and Coastal Fisheries*, 13(3), 253–
 493 262. <https://doi.org/10.1002/mcf2.10155>

494 Pacific Islands Regional Office (PIRO). (2020). *Essential Fish Habitat in Hawai'i* (p. 5). National
 495 Oceanic and Atmospheric Administration. [https://media.fisheries.noaa.gov/dam-migration/efh-](https://media.fisheries.noaa.gov/dam-migration/efh-hawaii-brochure-rebuild-for-web.pdf)
 496 [hawaii-brochure-rebuild-for-web.pdf](https://media.fisheries.noaa.gov/dam-migration/efh-hawaii-brochure-rebuild-for-web.pdf)

497 Parrish, F. A. (1989). Identification of habitat of juvenile snappers in Hawaii. *Fishery Bulletin*, 87(4),
 498 1001–1005.

499 Plymouth Marine Laboratory. (2020). *ESA CCI Ocean Colour Product 1997-2020*.
 500 <https://coastwatch.pfeg.noaa.gov/erddap/info/pmlEsaCCI42OceanColor8Day/index.html>

501 R Core Team. (2021). *R: A language and environment for statistical computing*. R Foundation for
 502 Statistical Computing. <https://www.r-project.org/>

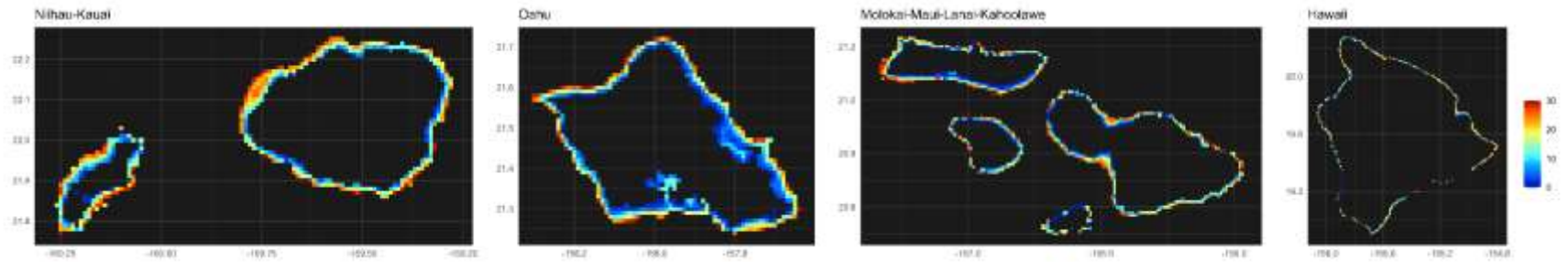
503 Shanmugam, P. (2011). A new bio-optical algorithm for the remote sensing of algal blooms in complex
 504 ocean waters. *Journal of Geophysical Research: Oceans*, 116(C4).

505 Tanaka, K. R., Belknap, S. L., Homola, J. J., & Chen, Y. (2017). A statistical model for monitoring shell

- 506 disease in inshore lobster fisheries: A case study in Long Island Sound. *Plos One*, 12(2), e0172123.
507 <https://doi.org/10.1371/journal.pone.0172123>
- 508 Tanaka, K. R., Chang, J.-H., Xue, Y., Li, Z., Jacobson, L., & Chen, Y. (2018). Mesoscale climatic
509 impacts on the distribution of *Homarus americanus* in the US inshore Gulf of Maine. *Canadian*
510 *Journal of Fisheries and Aquatic Sciences*, 18(July), 1–58.
- 511 Thorson, J. T. (2019). Guidance for decisions using the Vector Autoregressive Spatio-Temporal (VAST)
512 package in stock, ecosystem, habitat and climate assessments. *Fisheries Research*, 210, 143–161.
513 <https://doi.org/10.1016/j.fishres.2018.10.013>
- 514 Thorson, J. T., Shelton, A. O., Ward, E. J., & Skaug, H. J. (2015). Geostatistical delta-generalized linear
515 mixed models improve precision for estimated abundance indices for West Coast groundfishes.
516 *ICES Journal of Marine Science*, fsu243.
- 517 Tweedie, M. C. K. (1984). An index which distinguishes between some important exponential families.
518 *Statistics: Applications and New Directions*. In J. K. Ghosh & J. Roy (Eds.), *Proceedings of the*
519 *Indian Statistical Institute Golden Jubilee International Conference* (pp. 579–604). Indian Statistical
520 Institute.
- 521 Waldeck, D. A., & Buck, E. H. (2001). *The Magnuson-Stevens Fishery Conservation and Management*
522 *Act: Reauthorization issues for the 107th Congress*.
- 523 Western Pacific Regional Fishery Management Council (WPRFMC). (2021). *WPRFMC Five-year*
524 *Research Priorities under the MSRA 2020-2024* (p. 24). [https://www.wpcouncil.org/wp-](https://www.wpcouncil.org/wp-content/uploads/2022/01/2021-09-27-MSRA-Research-Priority-2020-2024.pdf)
525 [content/uploads/2022/01/2021-09-27-MSRA-Research-Priority-2020-2024.pdf](https://www.wpcouncil.org/wp-content/uploads/2022/01/2021-09-27-MSRA-Research-Priority-2020-2024.pdf)
- 526 Western Pacific Regional Fishery Management Council (WPRFMC). (2011). Hawaii Bottomfish
527 Essential Fish Habitat Appendices Agenda Item 10E2(2). *152nd Council Meeting*, 110.
- 528 Wikle, C. K., Zammit-Mangion, A., & Cressie, N. (2019). Spatio-Temporal Statistics with R. In *Spatio-*
529 *Temporal Statistics with R*. <https://doi.org/10.1201/9781351769723>
- 530 Zuur, A. F., Ieno, E. N., & Smith, G. M. (2007). *Analysing Ecological Data* (M. Gail, K. Kickeberg, J.
531 Samet, A. Tsiatis, & W. Wong (eds.)). Springer Science & Business Media.

532

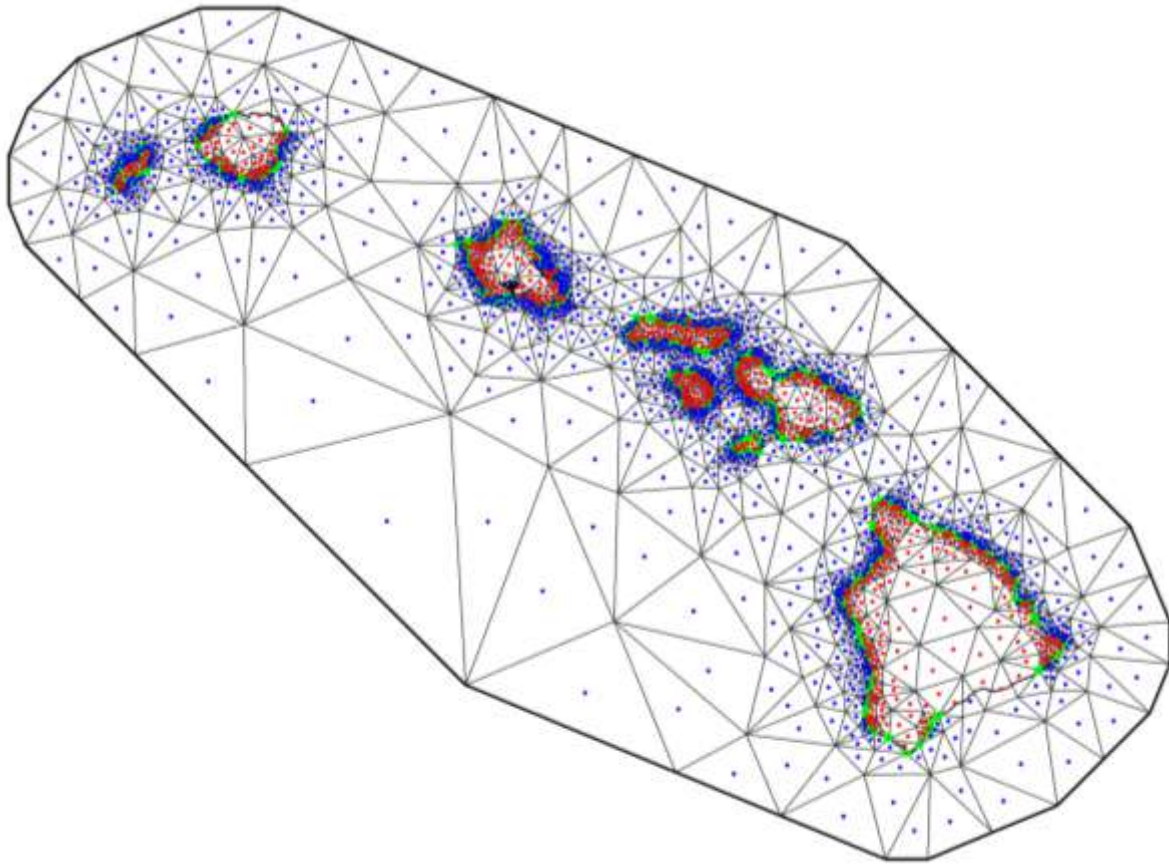
533 **Supplemental materials**



534

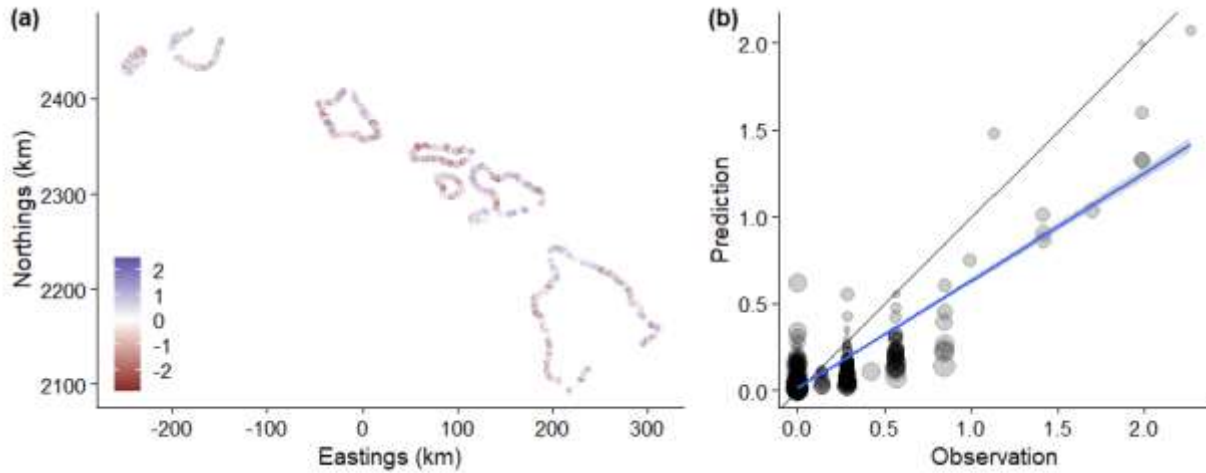
535 **Figure S 1. Bathymetric profiles of *Aprion virescens* density model domain within the Main Hawaiian Islands. Bathymetric data were drawn from**
536 **NOAA Coastal Relief Model, 3 arc second, Vol. 10.**

DRAFT



537

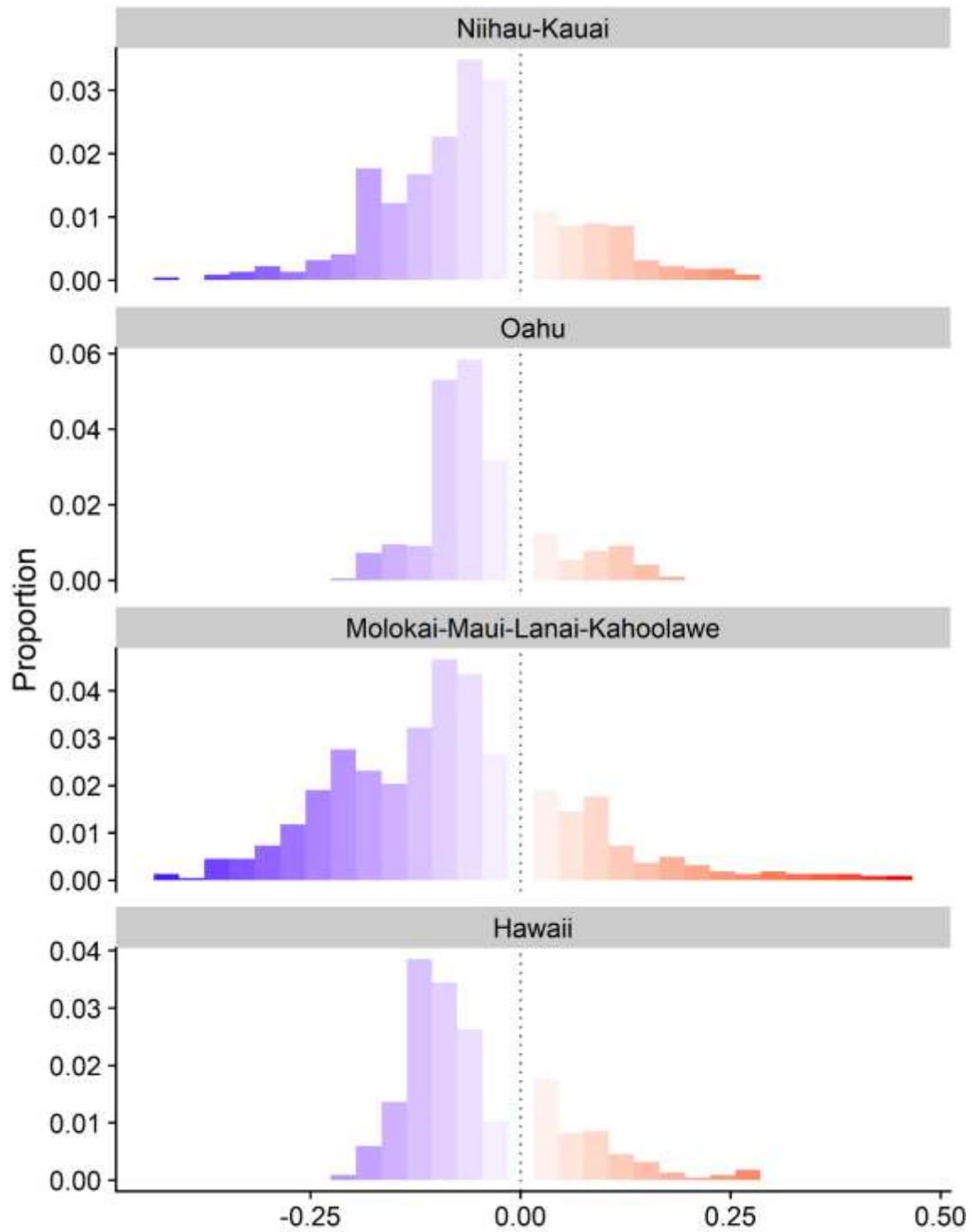
538 **Figure S2. Triangulated mesh covering the Main Hawaiian Islands region prepared with vertices at 500 knots**
539 **using the R INLA package. Axis units are in km based on UTM Zone 4 projection. Polygons with blue points**
540 **represent spatial domains considered for spatial autocorrelations in the spatiotemporal generalized linear**
541 **mixed model calibration process. Polygons with green dots represent land masses and were not included in**
542 **the spatial autocorrelations in the spatiotemporal generalized linear mixed model calibration process.**



543

544 Figure S 3. (a) Graphical summary of model residuals for the season-, stage-, and sex-aggregated *Aprion*
545 *virescens* generalized additive mixed modelling effort, and (b) observed versus predicted plots complemented
546 by linear regression lines. The solid line represents the 1:1 line and an ideal model performance.

DRAFT



547

548 **Figure S4. Spatially aggregated changes in *Aprion virescens* log density (2010-2019) within selected regional**
 549 **groups.**